16th ICAAR
LISBOA 2020-2022

16th International Conference on
Alkali-Aggregate Reaction in Concrete
Lisboa | LNEC | Portugal | 31 May - 2 June 2022
http://icaar2020-2022.lnec.pt

Prediction of the structural behavior of Bemposta dam (Portugal), affected by concrete swelling

Ivo Dias (1), António Lopes Batista (2), Rodolfo Rebelo (3)

(1) National Laboratory for Civil Engineering (LNEC), Lisbon, Portugal, idias@lnec.pt

(2) National Laboratory for Civil Engineering (LNEC), Lisbon, Portugal, albatista@lnec.pt

(3) Faculty of Sciences and Technology, New University of Lisbon (FCT/UNL), Portugal, rodolfoprebelo@gmail.com

Abstract

This paper presents the case study of the Bemposta dam, a hollow arch-gravity structure, whose concrete is affected by moderate expansive alkali-silica reactions.

To interpret the dam behavior and the effects of the expansive reactions, a structural model was developed, considering the evolution of the concrete properties, including creep and relaxation, and the evolution of the main actions, namely the hydrostatic pressure, the temperature variations and the expansions. The temperature variations in the dam's body were computed using a thermal model, considering the air and the water temperatures and the solar radiation on the dam's external surfaces.

A remarkable adjustment was obtained between the structural model and the monitored displacements, which allowed to validate the numerical models. The obtained results show that the swelling effects are already dominant on the dam behavior, both in terms of the horizontal and vertical displacements and in terms of the stress fields.

Based on the developed models and on two estimates for the expansion's evolution, an optimistic one, in which the expansions stabilize in the short term, and a pessimistic one, in which the remaining potential for expansion is still significant, two scenarios were established that enclose the behavior of the dam for the next 20 years.

Keywords*: Bemposta dam; monitoring; concrete swelling (ASR); finite element method; thermal analysis; structural analysis.*

1.   INTRODUCTION

1.1   Main characteristics of Bemposta dam

The Bemposta dam is a hollow arc-gravity structure, poured into the central blocks (Figure 1.1), located in the international section of the Douro River, downstream of the Picote dam and upstream of the Spanish dam of Aldeadavila. It is 87 m high and is founded on a rocky massif made up of granites and migmatites. The dam was completed in 1964, and granite aggregates were used in the concrete mix. The painting of the blocks and concrete structures on the right bank, downstream, was carried out as part of the architectural intervention in the works to strengthen the power of the hydroelectric plant, completed in 2011 (Figure 1.1).

The dam is operated by Engie and has been regularly monitored by LNEC. The monitoring results show a behavior greatly influenced, in the last decades, by the effects of expansive reactions of concrete, of the alkali-silica type, which are still of moderate magnitude (about 300×10^{-6}).
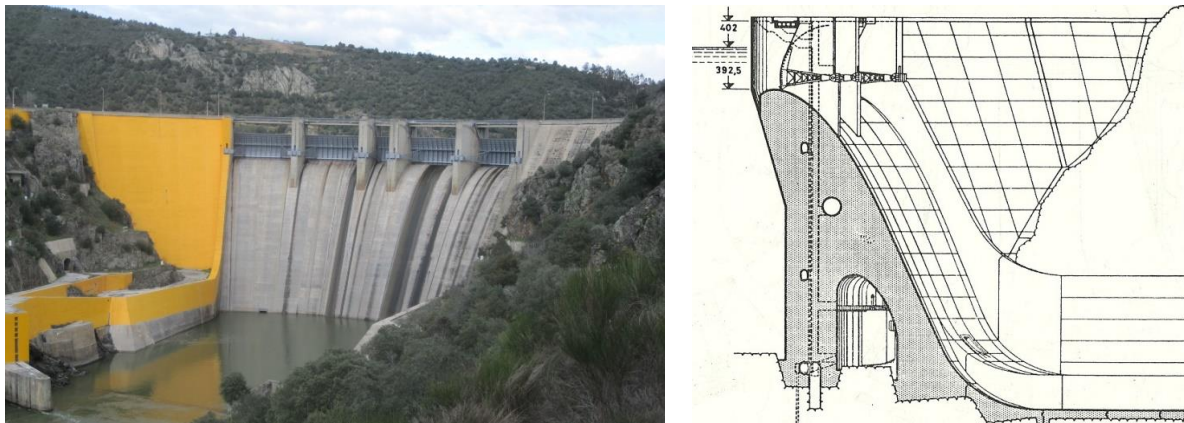
Figure 1.1: Bemposta dam. General view and central vertical cross-section

1.2 Evidence of the swelling phenomenon

Evidence of expansive phenomena was first identified in the 1990s, about 30 years after construction, through the observation of progressive displacements, vertical upwards (Figures 1.2) and radial upstream (Figure 3.2), vertical sliding in the contraction joints (at the crest level), closing of the side spans of the surface spillway (Figure 1.3) and increasing of the measured strains at some no-stress strain gauges. There are also deteriorated concrete surfaces in the galleries and diffuse cracking, of moderate expression, in specific areas of the galleries and on other surfaces (Figure 1.4).
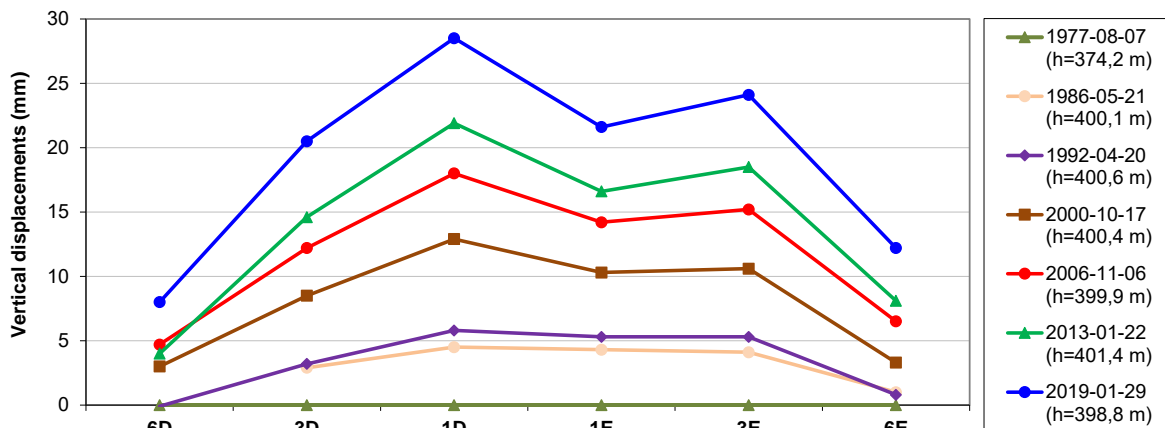

Figure 1.2: Crest vertical displacements observed by geodetic levelling, between 1977 and 2019 (positive upwards)

Regarding the vertical displacements of the crest, the increase rate over the last 20 years is practically constant, being around 0.6 mm/year in the central zone of the dam (Figure 1.2). The average vertical strains, accumulated since 1977, are about 300×10^{-6}.

There are progressive radial displacements upstream, in the upper central area of the dam, observed by geodesic methods and by plumb lines, with values of about 25 mm, which corresponds to a practically constant variation rate in recent decades, of about 0.8 mm/year (Figure 3.2). The closing of the side spans of the surface spillway reaches about 20 mm (Figure 1.3). Values of this order of magnitude will not cause problems with the gates movement, but they can cause the early deterioration of the watertightness systems, if they are operated regularly during the rainy season.

In the no-stress strain gauges of the dam, the monitored values of the concrete free strains are homothetic with the annual thermal wave (maximum annual variations of about 200×10^{-6}), only registering a progressive permanent trend over time in some of them. The two vertical stress cells in operation (C2 and C4, in the central zone) do not indicate stress variations over time.
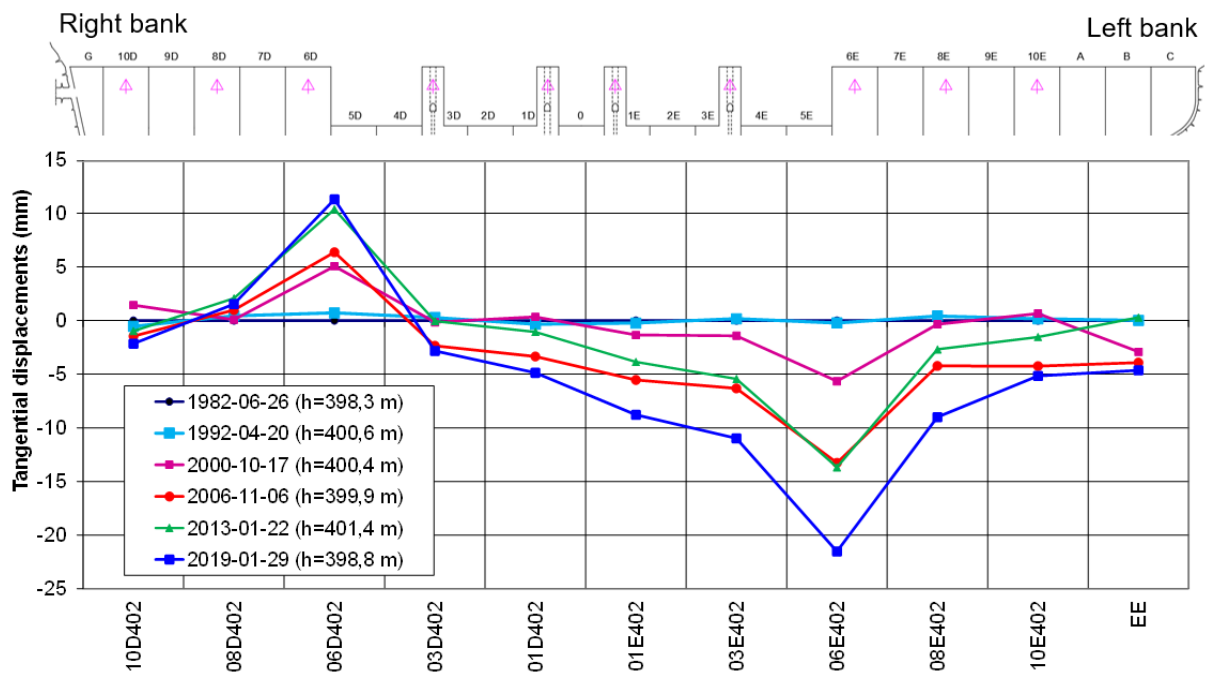
Figure 1.3: Tangential displacements observed by geodetic methods, near the crest (elevation 402.00 m), between 1982 and 2019 (positive to the left bank)

Figure 1.4: Map cracking at the top of the left abutment (left image) and on the right surface of pier 1D, upstream (right image) (photos taken in June 2019)

1.3 Scope of the paper

A study was recently carried out to interpret the observed behavior of the dam and to predict its behavior for the next decades [1]. It was intended to better understand the effects of the expansive action, including the stress fields in the dam. The temperature variations in the dam body were calculated with a thermal model that considered the air and water temperatures on the dam's outer surfaces and the effects of the solar radiation. The structural model considered the time evolution of the main actions (hydrostatic pressure, temperature variations and expansions) and of the concrete properties, having been analysed in a viscoelastic regime, to consider the creep and relaxation of the concrete. The expansions were estimated from the monitoring results, considering the thermal effects on the kinetics of chemical reactions. It was also considered the influence of the stress state on the development of the structural expansions. The main results related to the interpretation of the dam observed behavior, until 2020, were presented in a recent paper [2]. This paper presents the prediction of the dam's structural behavior for the next 20 years.

2. NUMERICAL MODELS

2.1 Finite element mesh

The finite element mesh (Figure 2.1), used for the structural and thermal analyses, has a total of 8300 elements and 31181 nodal points, of which 2235 are hexahedral elements with 27 nodal points (dam and gates) and 6065 are tetrahedral with 10 nodal points (rock mass foundation). The gates were considered in a simplified way, just to enable the application of the hydrostatic pressure.
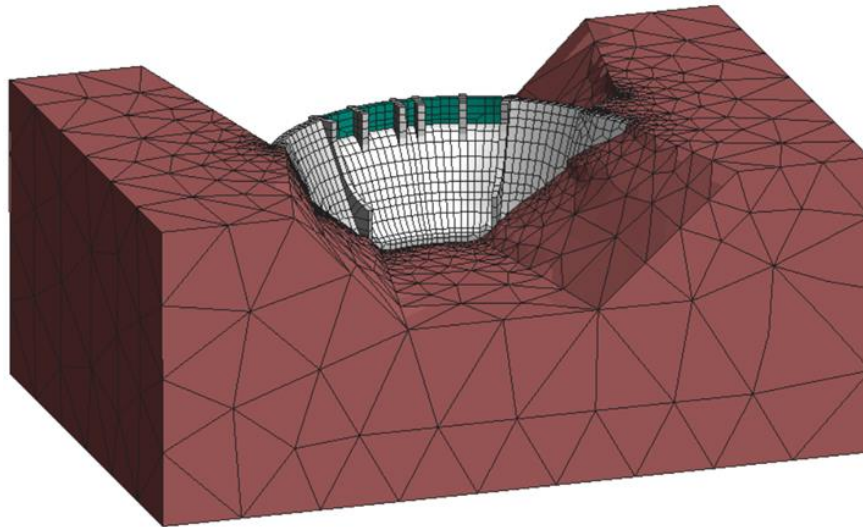

Figure 2.1: General view of the finite element mesh of the dam and its rock mass foundation

2.2 Thermal model

The temperature distribution across the dam body over time was computed by using a finite element code developed at LNEC [3] that solves the transient heat conduction equation (also known as Fourier's law), considering the air and water temperatures and the solar radiation in the external dam surfaces.

The air and water temperatures were represented by sinusoidal waves of annual period (1), where T_m is the average annual temperature, S_a is the semi-amplitude and ϕ is the number of days between the beginning of the year and the day of the highest temperature.

$$T(t) = T_m + S_a \cos\left(\frac{2\pi}{365}\,(t - \phi)\right) \tag{1}$$

The wave parameters were determined numerically by the least square method. For the air the adjusted wave curve is characterized by a mean annual temperature of 15.0 ºC and a semi-amplitude of 8.6 ºC. For the water reservoir, the temperature variation through depth was adjusted considering the monitoring values in 4 thermometers, located at different depths on the upstream face (Figure 2.2).
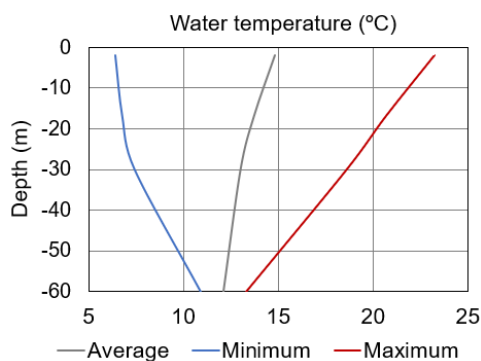
Location	T_m (ºC)	S_a (ºC)	ϕ (days)
Air	15.0	8.6	208
Reservoir (elevation 400 m)	14.8	8.4	222
Revervoir (elevation 385 m)	13.8	7.0	230
Reservoir (elevation 357 m)	12.3	5.5	235
Reservoir (elevation 342 m)	12.1	1.2	261

Figure 2.2: Parameters of the annual thermal waves of air and reservoir water temperatures

On the model boundaries in contact with the air convective heat transfer conditions were considered and as well the effects of the solar radiation, while the water temperature was directly prescribed on the nodal points of the surfaces in contact with the reservoir water. For the time domain an hourly discretization was used, which allows to model properly the solar radiation effects.

No specific tests were performed for characterizing the thermal properties of the concrete, being considering the following values, which correspond to average values for the concrete of dams: thermal conductivity $k = 2.6 \, W.m^{-1}.K^{-1}$; specific heat capacity $c = 920 \, J/(kg.K)$; convection coefficient $h_c = 25 \, W.m^{-2}.K^{-1}$; and absorption coefficient $a = 0.65$. For the concrete thermal expansion coefficient was considered $\propto_c = 1.2 \times 10^{-5} \, /°C$.

Figure 2.3 presents a comparison between the calculated temperatures and the values observed in the thermocouples embedded in the dam body, at an elevation of 385.0 m of block 6E, ordered from downstream to upstream. All the plots show that the calculated values adjust well to the observed values. The average temperature of the downstream face is about 5°C higher than the average temperature of the upstream face, because the average air temperature is higher than the average water temperature and also because of the effects of the solar radiation.
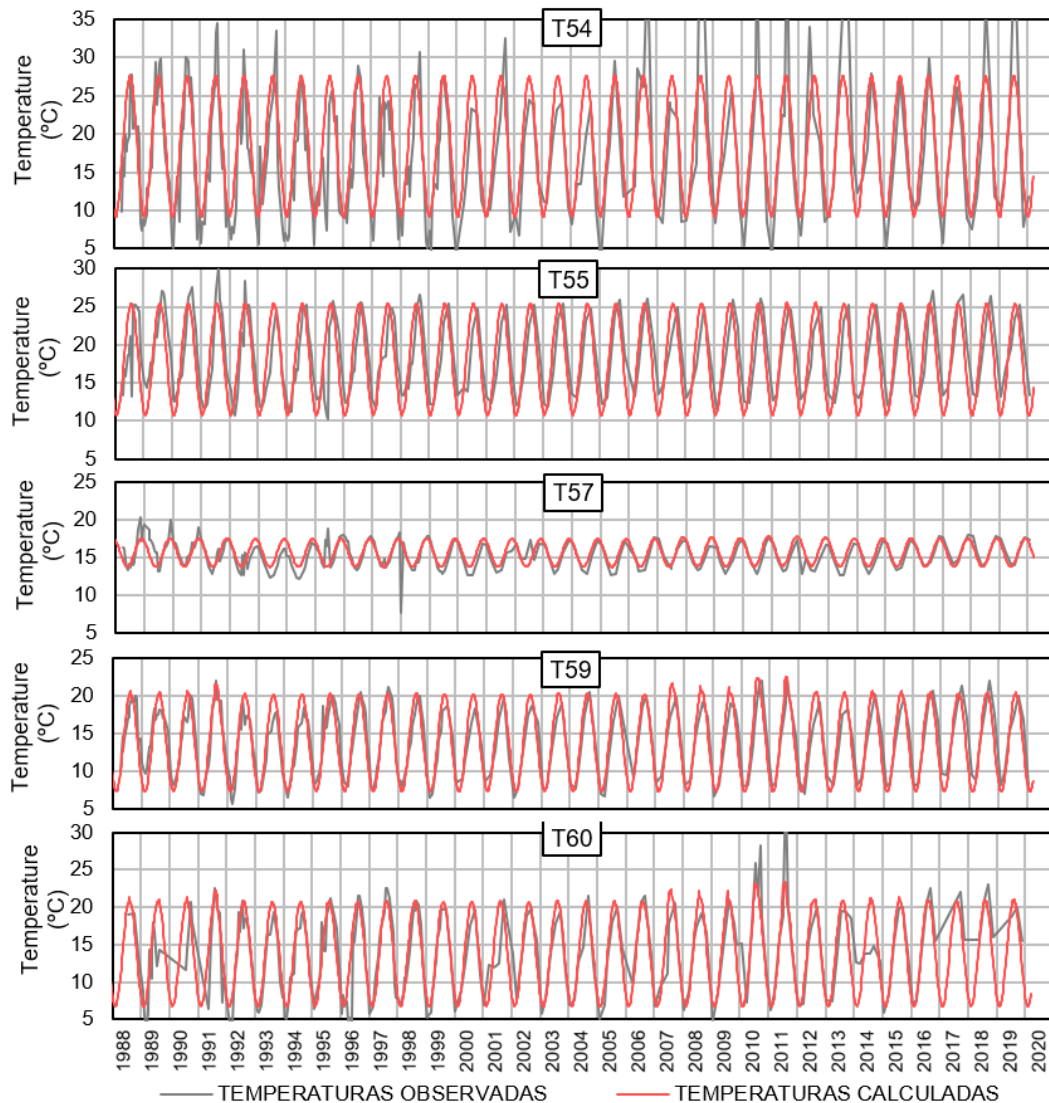

Figure 2.3: Comparison between computed and monitored temperatures in the thermocouples at an elevation of 385.0 m of block 6E, ordered from downstream to upstream

2.3 Concrete free swelling estimation

The concrete free swelling model assumes that the structural expansion growth depends on the uncoupled effects of the temperature g_T, the humidity g_H and the stress state g_σ, according to the following equation [4]:

$$\varepsilon_{exp}(H, T, \sigma, t) = \varepsilon_{exp,\infty}\, \xi_{exp}(t)\, g_H(H)\, g_T(T)\, g_\sigma(\sigma) \tag{2}$$

where $\varepsilon_{exp,\infty}$ is the long-term expansion (for a reference temperature T_{ref} and relative humidity of 100%) and ξ_{exp} is a function representing the time evolution of the expansive reaction, varying from 0, for the initial instant of time ($\xi_{exp}(t_0) = 0$), and 1, when the reaction has finished ($\xi_{exp}(t_\infty) = 1$). For ξ_{exp} is used an exponential sigmoid function, that has a profile similar to the curves obtained in laboratorial tests,

$$\xi_{exp}(t) = 1 - e^{-\frac{t^n}{\beta}} \quad ; \quad \beta = \frac{n}{n-1}(t_{hs})^n \tag{3}$$

where t represents time (in days), t_{hs} is the age (in days) corresponding to the curve inflection point and n is a real number that affects the curve shape.

The adopted function for $g_T(T)$ is,

$$g_T(T) = e^{6000\left(\frac{1}{T_{ref}} - \frac{1}{T}\right)} \tag{4}$$

in which T is the temperature (in Kelvin).

The function $g_H(H)$ was intuitively considered by dividing the dam in three different zones (Figure 2.4), where the Zone A, that is near the upstream face, has higher free swelling, and Zone C has lower swelling, since the cavity breaks the water flux throughout the dam concrete, from the upstream face.

The free swelling curves estimated until 2020 (Figure 2.4), for a reference temperature $T_{ref} = 14.5\ ^\circ C$, have the same long-term value of 600x10^{-6}. The curves parameters (Table 2.1) were estimated from the strains measured in the no-stress strain gauges (influenced by internal humidity conditions, which dictated the considered dam zoning), from the observed horizontal and vertical displacements of the dam, and also from results obtained with numerical simulations.
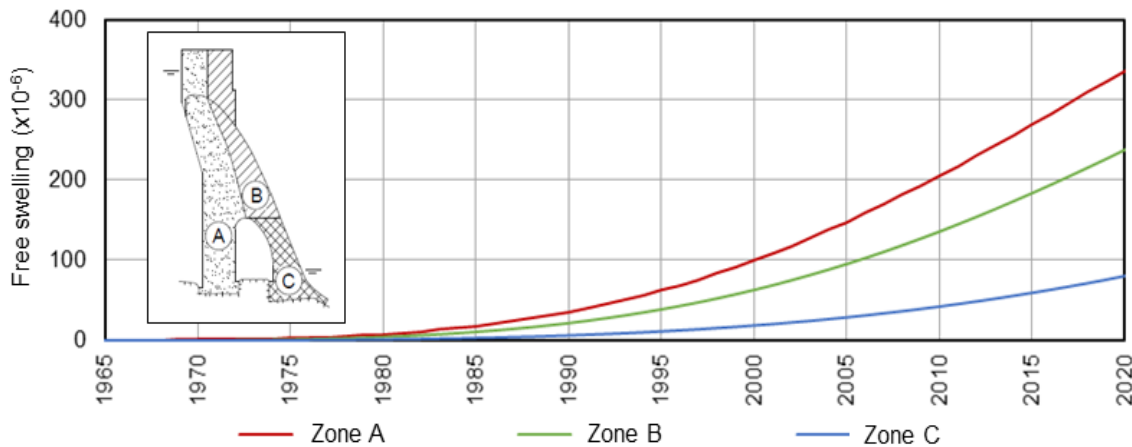

Figure 2.4: Zoning and evolution over time of the free swelling strains in the dam's body for the reference temperature of 14.5ºC

Table 2.1: Parameters of the curves of the free expansion evolution (3), for the reference temperature of 14.5ºC

Parameter	Zone A	Zone B	Zone C
n	3.5	3.5	3.5
t_{hs} (days)	20000	23000	33000
ε_∞ (x10^{-6})	600	600	600

The function $g_\sigma(\sigma)$ is determined from the exponential curve plotted in Figure 2.5, that was adjusted in LNEC to the experimental results obtained by Clayton [5] and Larive [6]. The factor g_σ was considered independently in the three principal stress directions.
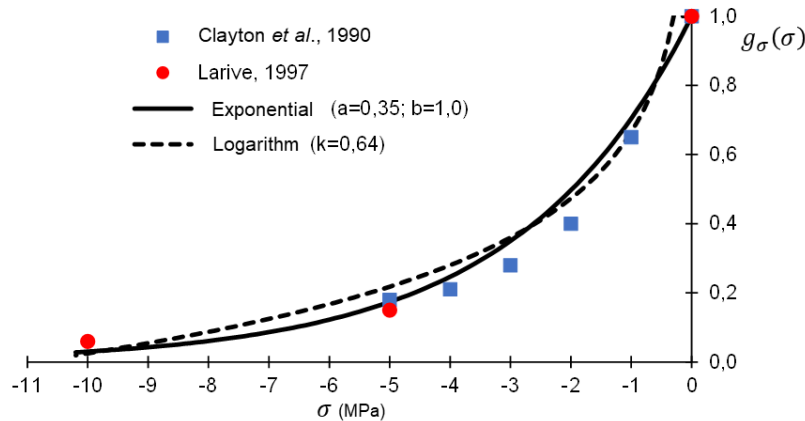

Figure 2.5: Influence of the stress field on the swelling development (taken from [4])

The free swelling computed is heterogeneous along the dam body, since the zones with higher temperatures have more expansions, while the structural expansions are also anisotropic, since the more compressed directions have less expansions.

2.4 Structural model

The structural modelling was performed by using a finite element code, that is being developed at LNEC [7-10]. A homogeneous continuous model was used since the movements at the contraction joints are very small (the concrete swelling also contributes for closing these joints).

The model considers the main loads applied to the dam, namely the concrete dead weight, the hydrostatic pressure on the upstream face, the concrete temperature variations in the dam's body and the concrete swelling. For the time domain a weekly temporal discretization was used.

The concrete dead weight was applied by means of vertical body forces (γ_c=24 kN/m³). The water pressure was simulated by surface loads, applied on the upstream face of the dam and on the spillway gates (γ_w=10 kN/m³), considering a weekly discretization over time (Figure 2.6). The concrete temperatures and expansions were computed by using the thermal model and the expansive action model, respectively.
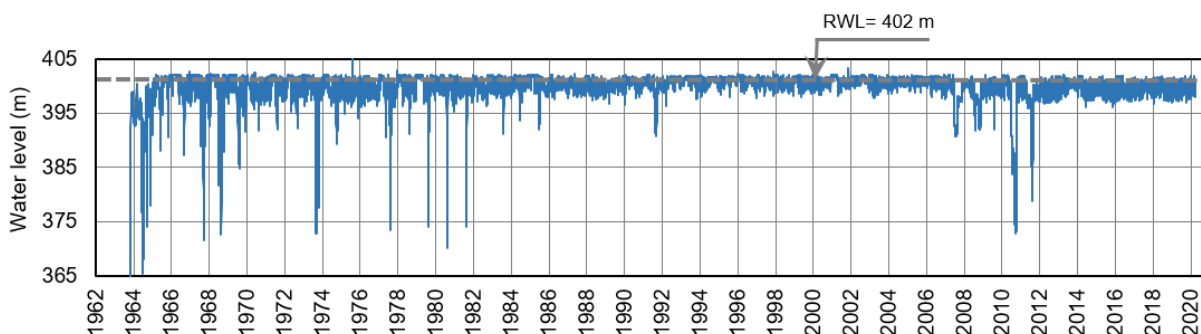

Figure 2.6: Reservoir level since 1963 until 2020

The rock mass foundation behavior was considered linear elastic with modulus of deformability of 15 GPa and Poisson ratio of 0.2. The deformability of the concrete of the dam body was simulated by a viscoelastic model, characterized by Poisson ratio of 0.2 and by the Bažant-Panula creep law,

$$J(t,t_0) = \frac{1}{43.3}(1 + 4.5(t_0^{-0.40} + 0.05)(t - t_0)^{0.12}) \text{ (GPa}^{-1}) \tag{5}$$

3. ANALYSIS AND PREDICTION OF THE STRUCTURAL BEHAVIOR

The results computed by the structural model, together with the data provided by the dam monitoring system until 2020, allows to validate the thermal and the structural models, namely with respect to the type of models, the material properties and the main actions. The results show that the swelling effects are already dominant on the dam behavior, both in terms of the horizontal and vertical displacements and in terms of the stress fields.

To forecast the dam's behavior for the next 20 years (since 2020 until 2040), a set of hypotheses were considered. The reservoir water level was considered constant in time and equal to the average water level in the last years, approximately 400 m (Figure 2.6). The curves for the annual temperature variations in the air and in the reservoir water remain the ones of Figure 2.2. Relative to the concrete swelling evolution since 2020, two scenarios were considered: an optimistic one, in which the expansions stabilize in the short term, and a pessimistic one, in which the remaining potential for expansion is significant (Figure 3.1). Table 3.1 shows the parameters of the free expansion curves, for the reference temperature of 14.5ºC, for the two considered scenarios.
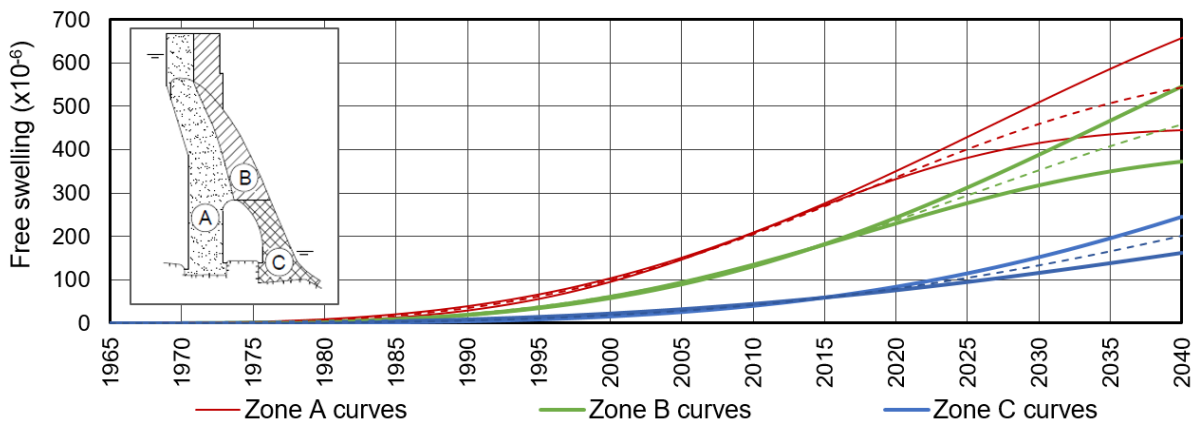

Figure 3.1: Free swelling evolution until 2040 for the optimistic and the pessimistic scenarios

Table 3.1: Parameters of the free expansion curves since 2020, for the reference temperature of 14.5ºC, for the pessimistic and optimistic scenarios

Zone	A		B		C	
Scenario	Pessimistic	Optimistic	Pessimistic	Optimistic	Pessimistic	Optimistic
n	3.3	4.0	3.6	3.8	4.0	3.0
t_{hs} (days)	23500	18000	26200	20000	33000	30500
Long-term free swelling $(T_{ref} = 14.5\,°C)$	900×10^{-6}	450×10^{-6}	900×10^{-6}	400×10^{-6}	750×10^{-6}	400×10^{-6}

Figure 3.2 shows the evolution of the radial displacements since the first filling of the reservoir until 2020, monitored in the central plumb line and by geodetic methods near the crest, along with the values computed with the numerical model until 2040, considering the combined loads of the dead weight, water pressure, swelling and their delayed effects, for the two considered scenarios. The good agreement between the computed and observed results, until 2020, is remarkable. It is noticed that after 1990 the dam behaviour ceased to be reversible, being dominated by the swelling effects. In 2040 the displacements will reach values of about 30 mm and 50 mm, upstream, for the optimistic and pessimistic scenarios, respectively.
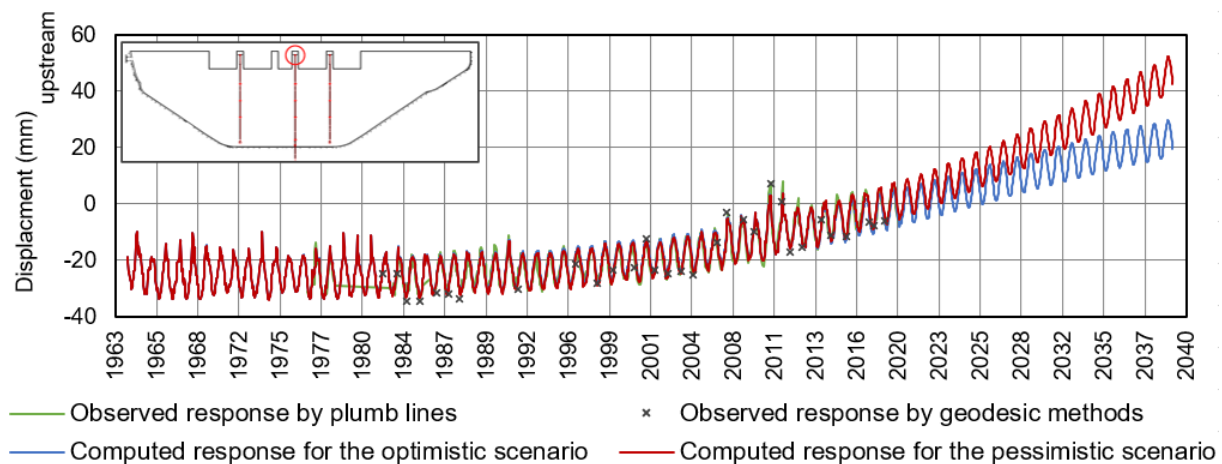
Figure 3.2: Central cantilever radial displacements near the crest, measured on the central plumb line and by geodetic methods until 2020 and computed until 2040 for the optimistic and the pessimistic scenarios

Figure 3.3 presents the evolution of the vertical displacement at a central point of the crest. It can be noticed that the computed vertical displacements compare well with those observed by the geometric levelling, until 2020. The irreversible displacements are entirely due to swelling effects, since 1990. In 2040 the vertical displacements will reach values of about 30 mm and 40 mm, upwards, for the optimistic and pessimistic scenarios, respectively.
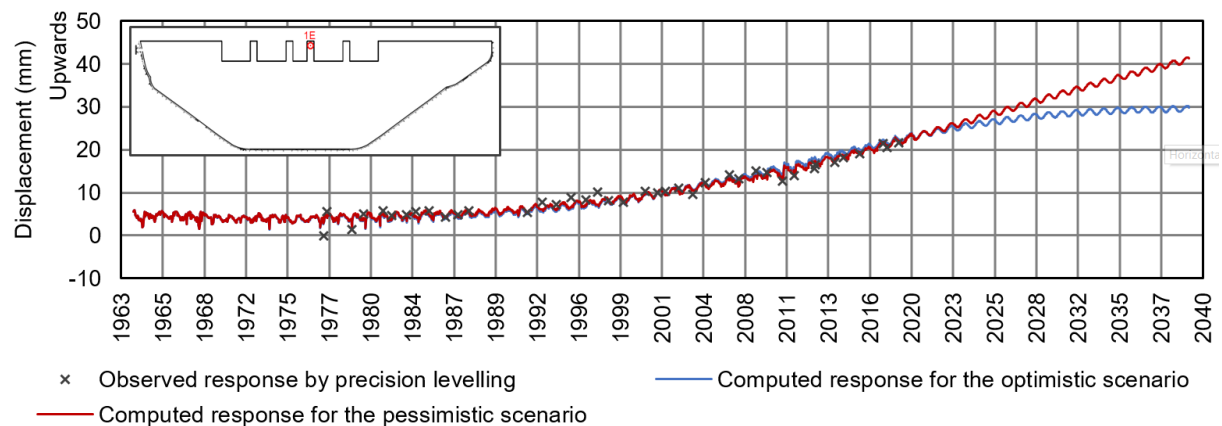

Figure 3.3: Vertical displacements at a central point of the crest, measured by geometric levelling until 2020 and computed until 2040 for the optimistic and the pessimistic scenarios

Figure 3.4 presents the principal stresses on the upstream and downstream faces, computed in 2020, due to the combined loads of the dead weight, hydrostatic pressure and swelling, as well as their delayed effects. The stress field is generally compressive except for some zones of the downstream face, where tensile stresses occur. In compression, the maximum values occur in the upstream face, near the foundation connection, reaching values of about 10 MPa on the right bank. On the downstream face, the compressive stresses are also high near the lateral bearings, with values of about 6 MPa in both sides. The maximum tensile stresses occur on the downstream face near the banks, are approximately normal to the foundation surface and reach values of about 2.7 MPa in the left side. Due only to swelling (Figure 3.5), the stress field is also generally compressive, but in the downstream leg and in the abutments, there are tensile stresses that reach about 3.5 <MPa.

Figures 3.6 and 3.7 show the predicted stress fields for 2040 for the optimistic and the pessimistic scenarios, respectively. The maximum compressive stresses will remain increasing, reaching values ranging from 13 MPa to 18 MPa for the optimistic and the pessimistic scenario, respectively. The tensile stresses will also increase, reaching values between 3.0 MPa (optimistic scenario) and 4.2 MPa (pessimistic scenario) on the downstream face of the left abutment.
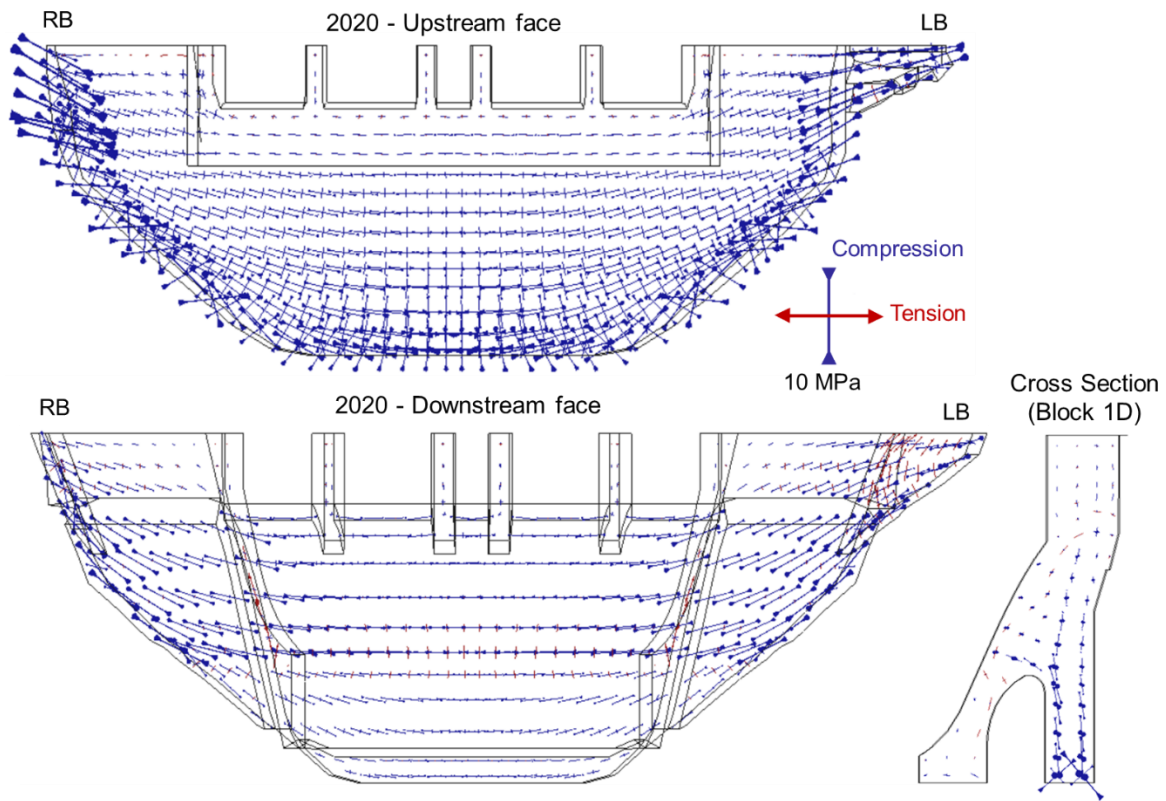
Figure 3.4: Principal stresses on dam faces and in the cross section of block 1D computed in 2020, due to the combined loads of the dead weight, hydrostatic pressure and swelling
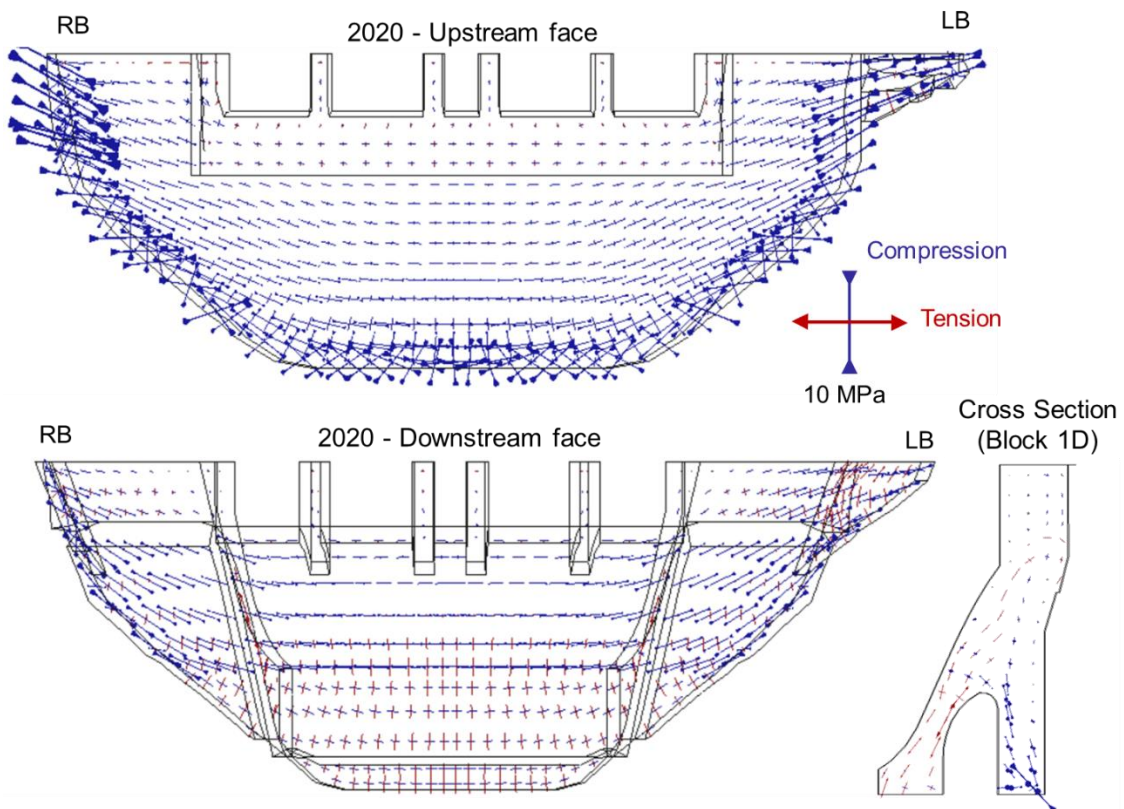

Figure 3.5: Principal stresses on dam faces and in the cross section of block 1D computed in 2020, due to swelling
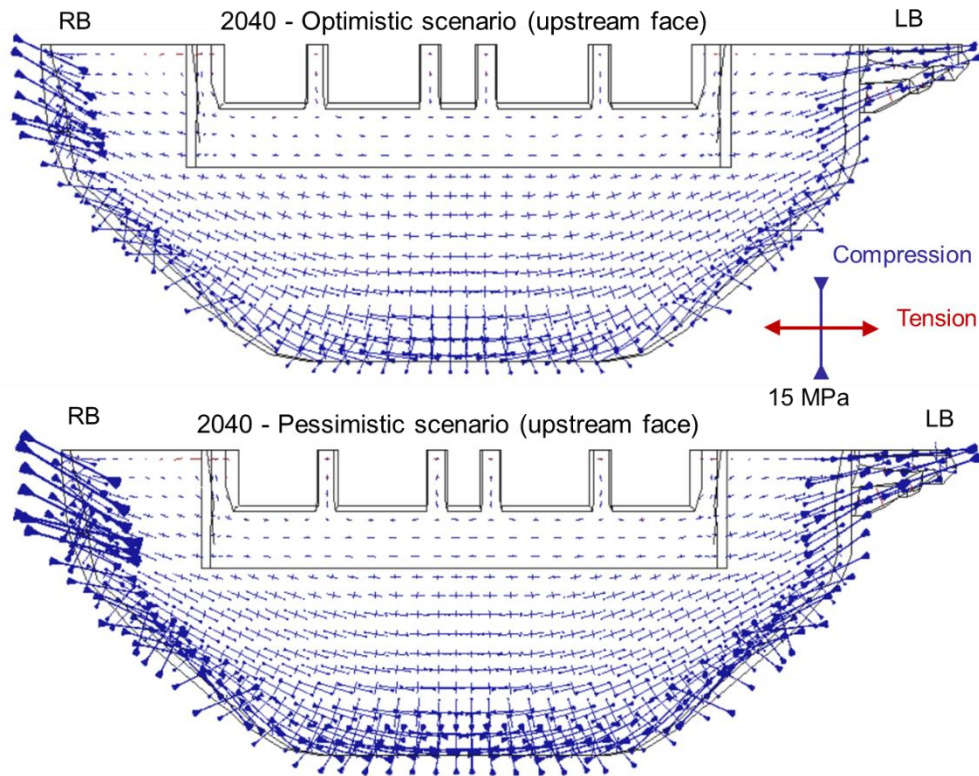
Figure 3.6: Principal stresses on the upstream face predicted for 2040, due to the combined loads of the dead weight, hydrostatic pressure and swelling, for the optimistic and the pessimistic scenarios
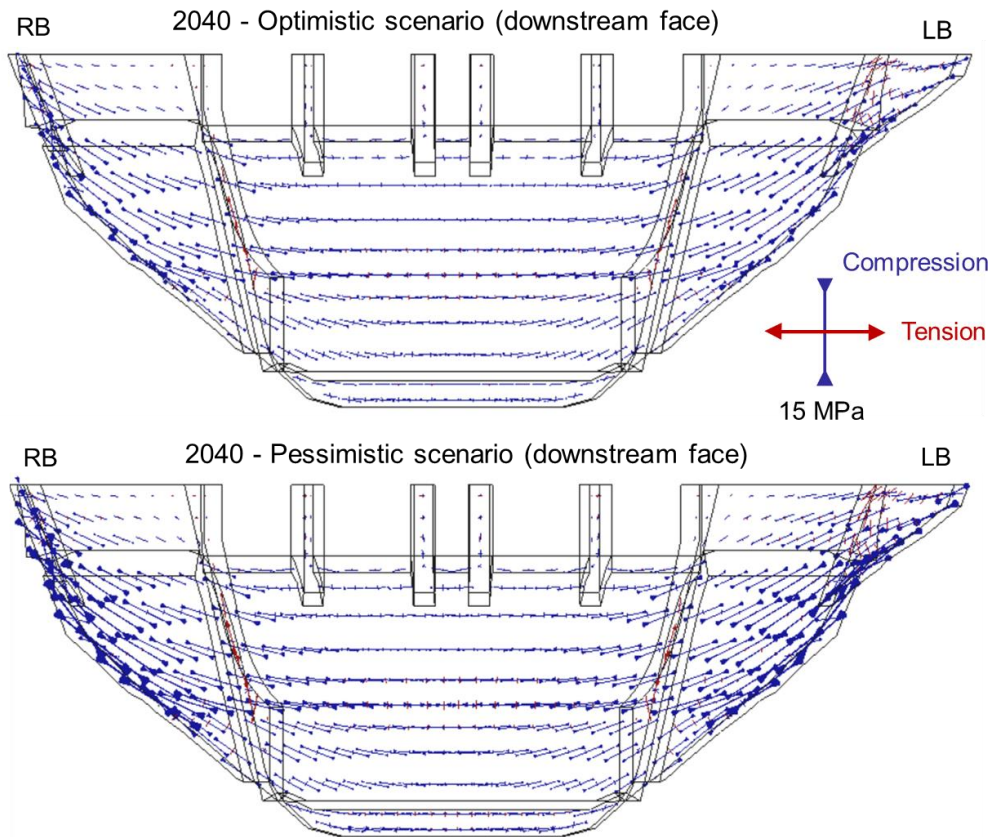

Figure 3.7: Principal stresses on the downstream face predicted for 2040, due to the combined loads of the dead weight, hydrostatic pressure and swelling, for the optimistic and the pessimistic scenarios

4.   FINAL REMARKS

The monitored values and the numerical results, in terms of displacements, showed a good agreement until 2020, attesting the adequacy of the models used to simulate the Bemposta dam's behaviour. These models were used, in a second stage, to predict the dam's behavior for the next two decades, considering two scenarios for the swelling evolution, one pessimistic and one optimistic. For both scenarios the expansions will continue to have a central role in the dam's behavior.

The stress fields have a higher relevance at the abutment bearings, near the crest. In these zones, maximum stresses of about 10 MPa (compression) and 2,7 MPa (tension) were computed in 2020. For 2040, the maximum compressive stresses on the upstream face of the right abutment can reach values ranging from 13 MPa to 18 MPa, for the optimistic and pessimist scenario, respectively. Since in the worst-case scenario the stress estimate will be about 60% of the average concrete strength (about 30 MPa), the stress evolution in this zone of the dam should deserve special attention in the dam's structural safety control. Tensile stresses will also remain increasing, being therefore expected that some cracking might occur, in some limited areas of the downstream face, near the lateral bearings.

ACKNOWLEDGMENT

REFERENCES

[1]   Rebelo R (2021) Study of the structural behavior of arch-gravity dams affected by concrete swelling. Application to Bemposta dam *(in Portuguese)*. Master thesis, Faculdade de Ciências e Tecnologia, Universidade Nova de Lisboa, Lisbon.

[2]   Rebelo R, Dias IF, Batista AL (2021) Identification and modeling of the concrete swelling effects in the Bemposta dam *(in Portuguese)*. Reabilitar & Betão Estrutural 2020, Lisbon.

[3]   LNEC (Leitão N) (2012) Thermal analysis of concrete dams: Environmental thermal actions *(in Portuguese)*. Report 185/2012, DBB/NMMF, Lisbon.

[4]   Batista A (2021) Structural management and rehabilitation of dams affected by concrete swelling reactions *(in Portuguese)*. Research program, LNEC, Lisbon.

[5]   Clayton N, Currie RJ, Moss RM (1990) The effects of alkali-silica reaction on the strength of prestressed concrete beams. The Structural Engineer, 68, N. 15, p. 287-292.

[6]   Larive C (1997) Apports combinés de l'expérimentation à la compréhension de l'alcali-réaction et de ses effets mécaniques. PhD thesis, École Nationale des Ponts et Chaussées, Paris, France.

[7]   Batista A (1998) Analysis of the behaviour over time of arch dams *(in Portuguese)*. PhD thesis, Instituto Superior Técnico, Lisbon.

[8]   Oliveira, S (2000) Models for analysing the behaviour of concrete dams considering cracking and the time effects. Damage formulation *(in Portuguese)*. PhD thesis, Faculdade de Engenharia da Universidade do Porto, Porto.

[9]   Piteira Gomes J (2007) Structural behaviour modelling of concrete dams subject to swelling reactions *(in Portuguese)*. PhD thesis, Faculdade de Ciências e Tecnologia, Universidade Nova de Lisboa, Lisbon.

[10]   Dias IF, Oliver J, Huespe AE (2012) Strain injection techniques in numerical modeling of propagating material failure. Monograph CIMNE M134. International Center for Numerical Methods in Engineering, Barcelona.